PCCP

Accepted Manuscript

ROYAL SOCIETY OF CHEMISTRY

www.rsc.org/pccp

Journal Name

ARTICLE TYPE

Cite this: DOI: 10.1039/xxxxxxxxxx

Exploring the Nature of the Excitation Energies in $[Re_6(\mu_3\text{-}Q_8)X_6]^{4-}$ Clusters: A Relativistic Approach†,‡

Walter A. Rabanal-León,[a] Juliana A. Murillo-López,[a,b] Dayán Páez-Hernández,[a] and Ramiro Arratia-Pérez[a,*]

Received Date
Accepted Date

DOI: 10.1039/xxxxxxxxxx

www.rsc.org/journalname

This contribution is a relativistic theoretical study to characterize systematically the main electronic transitions in a series of hexarhenium chalcogenide $[Re_6(\mu_3\text{-}Q_8)X_6]^{4-}$ clusters with the aim to understand: i) the terminal ligand substitution effect, ii) the substitution effect of the chalcogenide ion on the $[Re_6(\mu_3\text{-}Q_8)]^{2+}$ core, and finally iii) the significance of the spin-orbit coupling (SOC) effect on the optical selection rules. In all the cases, we found characteristic bands around 300-550 nm, where the band positions are directly determined by the terminal ligand. However, the SCN^-/NCS^- present a different nature of the orbitals involved on the electronic transitions, in comparison with the other studied terminal ligands, and are located in the near-infrared (NIR) region. All the bands are red-shifted as a consequence of the ligand contribution in the composition of the orbitals involved in the electronic excitations.

1 Introduction

Since their discovery at Rennes University in 1971,[1] chalcogenide transition metal (Mo and Re) clusters have been substantially studied due to the high stability of the octahedral $[M_6(\mu_3\text{-}Q_8)]^{2+}$ core,[2] their redox behaviour,[3–7] photophysical properties,[8–18] synthetic versatility and their capability to build functional multi-cluster supramolecular assemblies[19–24] with potential applications on the development of magnetic and optical devices.[13,18,25–29]

Particularly, the luminescence exhibited by the hexanuclear rhenium chalcogenide clusters was firstly predicted theoretically by Arratia-Pérez for the sulfide/selenide rhenium clusters,[30–32] this was made on the base of the electronic structure similarities with the well-known luminescent hexanuclear tungsten halide clusters $[W_6X_{14}]^{2-}$ and with the cluster contained in the superconducting Chevrel phases. The luminescent properties was experimentally corroborated by Yoshimura,[9] Batail,[10] and Holm.[11] They found that the luminescence of the $[Re_6(\mu_3\text{-}Q_8)X_6]^{4-}$ clusters occurs for excitation wavelengths in the range of its most intense absorption bands around 350-450 nm. Furthermore, it was found that the luminescence for these series of halide rhenium chalcogenide clusters shift to a longer wavelength when we move down to the halogen group and also that their emission spectra are analogous to the hexanuclear molybdenum(II) and tungsten(II),[3,4] which made these clusters were considered as promising lumophores for a wide range of light-based applications. The latest efforts to design novel luminescent materials are focused on the construction of framework structures containing the $[M_6(\mu_3\text{-}Q_8)]^{2+}$ build linker to incorporate red/near-infrared luminescence on the construction of functional materials.[20–24,26–29,33–35]

More recently, Arratia-Pérez and co-workers performed a deeply relativistic study related to the bonding nature and reactivity on a set of hexarhenium chalcogenide clusters with σ-donor and σ-donor/π-acceptor terminal ligands, they found in all cases an extensive ionic interaction (around 75%) among the core and the terminal ligands. It was concluded that the most stable clusters are those that present the stronger σ-donor terminal ligands, whereas the cluster stability starts to decrease when the π-acceptor effect will be stronger; this fact is directly related with the terminal ligand lability and the strong electrophilic character of the $[Re_6(\mu_3\text{-}Q_8)]^{2+}$ core.[36]

The aim of this work is to establish, from a theoretical point of view, the factors that control the photophysics of the $[Re_6(\mu_3\text{-}Q_8)X_6]^{4-}$ clusters; that means, identify and understand the consequences of the chalcogenide and the terminal ligand substitution on the optical properties, in order to modulate the luminescence in different regions of the spectra, specially on the red and near-infrared region.

[a] Universidad Andrés Bello, Facultad de Ciencias Exactas, Ph.D. Program in Molecular Physical Chemistry, Relativistic Molecular Physics (ReMoPhys) Group, Santiago, Chile. Tel/Fax: +56-2-2770-3352; E-mail: rarratia@unab.cl* (Corresponding Author)
[b] Universidad de Talca, Facultad de Ingeniería, Centro de Bioinformática y Simulación Molecular (CBSM), 2 Norte 685, Casilla 721, Talca, Chile.

† Electronic Supplementary Information (ESI) available: Calculated absorption spectra, electronic transitions characterization, molecular spinor density plots and electron density difference maps for all the $[Re_6(\mu_3\text{-}Q_8)X_6]^{4-}$ complexes at spin-orbit relativistic level. See DOI: 10.1039/b000000x/

‡ All the authors contribute equally to this work.

2 Computational Details

This contribution is based on the study of the spectroscopy properties of a series of Rhenium chalcogenide clusters with general formula $[Re_6(\mu_3\text{-}Q_8)X_6]^{4-}$, where Q are the S^{2-}, Se^{2-} and Te^{2-} chalcogenides and X are a set of, σ-donor or π-acceptor, terminal ligands as F^-, Cl^-, Br^-, I^-, CN^-, NC^-, SCN^-, NCS^-, OCN^- and NCO^- following the scheme depicted in Figure 1.

All this work were developed on the framework of the relativistic density functional theory (R-DFT) by using the Amsterdam Density Functional (ADF 2012.01) code,[37] where the scalar (SR) and spin-orbit coupling (SOC) relativistic effects were incorporated by means of a two-component Hamiltonian with the zeroth-order regular approximation (ZORA).[38,39] The molecular structures presented above were taken from a previous contribution from Arratia-Pérez and co-workers,[36] which are in good agreement with the experimental data reported.[2,40–43]

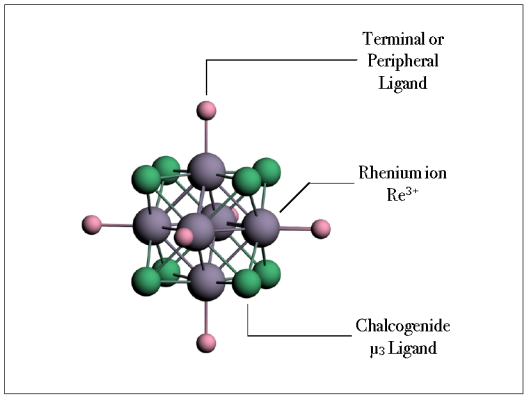

Fig. 1 Molecular model for the $[Re_6(\mu_3\text{-}Q_8)X_6]^{4-}$ cluster.

In order to calculate the absorption spectra of these molecules, the lowest one hundred excitation energies were computed using the time-dependent density functional theory (TD-DFT) at thescalar and spin-orbit relativistic level.[44,45] The excitation energies were calculated using the statistical average of orbital exchange-correlation model potential (SAOP).[46] Solvation effects were modeled by a conductor-like screening model for real solvents (COSMO)[47,48] using acetonitrile as solvent due to the availability of experimental data. The calculated absorption spectra were plotted by using Lorentzian weighted functions by the respective oscillator strengths with a peak width of 20 nm. Moreover, uncontracted all-electron triple-ζ quality Slater-type orbitals (STO) basis set augmented by two sets of polarization functions (TZ2P) were used for the all atoms,[49] under an double-valued octahedral (O_h^*) symmetry constraint, that means we change the framework from molecular orbitals to molecular spinors. Thus, the molecular spinors are taken to transform according to the octahedral extra irreducible representations. In our notation, these doubled-valued irreducible representations are related to the usual Bethe's notation as follows:

$$e_{1/2g,u} \leftrightarrow \Gamma_{6^\pm}; \quad e_{5/2g,u} \leftrightarrow \Gamma_{7^\pm}; \quad u_{3/2g,u} \leftrightarrow \Gamma_{8^\pm}$$

Here, the *e* and *u* extra-irreps correspond to two and four-fold symmetries, respectively.

The traditional irreducible representations of the single-group used in the present contribution can be translated as follows:

$$\begin{aligned} a_{1g} &= e_{1/2g};\ a_{2g} = e_{5/2g};\ e_g = u_{3/2g}; \\ t_{1g} &= e_{1/2g} \oplus u_{3/2g};\ t_{2g} = e_{5/2g} \oplus u_{3/2g}; \\ a_{1u} &= e_{1/2u};\ a_{2u} = e_{5/2u};\ e_u = u_{3/2u}; \\ t_{1u} &= e_{1/2u} \oplus u_{3/2u};\ t_{2u} = e_{5/2u} \oplus u_{3/2u} \end{aligned}$$

They were obtained as a consequence of the interaction of the single-valued irreducible representations with the spin-irreducible ($\gamma_{1/2}^{spin}$) representation. It should be clear that the SOC split the orbital degeneracy and breaks the optical selection rules. Moreover, for the octahedral point group, it is easy to obtain the double group symmetry allowed electronic transitions, resulting as:

$$\begin{aligned} &e_{1/2g} \leftrightarrow e_{1/2u}, \quad e_{1/2g} \leftrightarrow u_{3/2u}, \quad e_{1/2g} \leftrightarrow e_{5/2u}, \\ &u_{3/2g} \leftrightarrow e_{1/2u}, \quad u_{3/2g} \leftrightarrow e_{5/2u}, \quad e_{5/2g} \leftrightarrow u_{3/2u} \end{aligned}$$

These symmetry (and spin) allowed rules should be taken into account when assigning absorption and emission bands.

3 Results and Discussions

1) σ-donor Ligands

In the case of the halide terminal ligands (F^-, Cl^-, Br^- and I^-) and independently of the chalcogenide in the $[Re_6(\mu_3\text{-}Q_8)]^{2+}$ core (Q = S^{2-}, Se^{2-} and Te^{2-}), it is observed a red-shift when the halide terminal ligand becomes heavier (more labile), as can be observed in Figure 2 for the sulphide case.

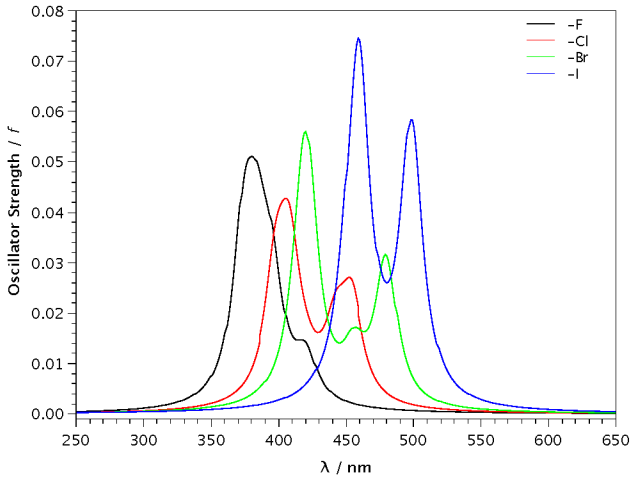

Fig. 2 Calculated excitation energies for the $[Re_6(\mu_3\text{-}S_8)X_6]^{4-}$ (X = F^-, Cl^-, Br^- and I^-) cluster series at spin-orbit relativistic level with the SAOP functional in acetonitrile solvent.

This red-shift for the halide series is directly related to the nature of the spinors involved in the main electronic transitions of their spectra. In all the cases, the electronic transitions occurs from molecular spinors centred in the core to spinors also centred in the core, but with a progressive increment of the terminal ligand contribution. In Table 1 is observed that the increment of the ligand contribution is as follows: I^- (22.41%) > Br^- (16.44%) > Cl^- (11.55%) > F^- (0.16%), this allow us to characterize these

Table 1 Excitation energies (eV), wavelengths (nm), oscillator strengths (*f*) and orbital assignation for the $[Re_6(\mu_3\text{-}S_8)X_6]^{4-}$ complexes (X = F^-, Cl^-, Br^-, I^-) at spin-orbit relativistic level with the SAOP functional in acetonitrile solvent.

Band	Energy	λ	f(x100)	Active MOs	%	Assignation
$[Re_6(\mu_3\text{-}S_8)F_6]^{4-}$						
a	3.31	374	0.9898	52 $u_{3/2g}$ → 53 $u_{3/2u}$ 52 $u_{3/2g}$ → 54 $u_{3/2u}$	62 25	Core - Core
b	3.23	383	0.7816	52 $u_{3/2g}$ → 53 $u_{3/2u}$ 52 $u_{3/2g}$ → 24 $e_{5/2u}$	70 18	
$[Re_6(\mu_3\text{-}S_8)Cl_6]^{4-}$						
a	3.11 (3.26†)	398	0.9111	56 $u_{3/2g}$ → 57 $u_{3/2u}$ 56 $u_{3/2g}$ → 25 $e_{5/2u}$	71 19	Core - Core + 11.55% Lig
b	3.03	408	0.7523	56 $u_{3/2g}$ → 57 $u_{3/2u}$ 56 $u_{3/2u}$ → 25 $e_{5/2g}$	74 14	MLCT
$[Re_6(\mu_3\text{-}S_8)Br_6]^{4-}$						
a	2.94 (2.80¶)	442	1.6855	65 $u_{3/2g}$ → 66 $u_{3/2u}$	86	Core - Core + 16.44% Lig
b	2.58	479	0.9588	65 $u_{3/2g}$ → 41 $e_{1/2u}$	97	MLCT
$[Re_6(\mu_3\text{-}S_8)I_6]^{4-}$						
a	2.69	459	2.1120	32 $e_{5/2u}$ → 75 $u_{3/2g}$ 74 $u_{3/2u}$ → 33 $e_{5/2g}$	74 16	Core - Core + 22.41% Lig
b	2.48 (2.44¶)	498	1.7835	74 $u_{3/2g}$ → 46 $e_{1/2u}$	95	MLCT

† Ref. [10]
¶ Ref. [19]

bands as intra-core electronic transitions with certain character of metal to ligand charge transfer (MLCT), instead of the experimental assignation as ligand to metal charge transfer (LMCT) (see Figures 3a and 3b). In the same way, it is observed an increment on the intensities (oscillator strength) of the bands due to the facility of the charge transfer phenomena on the soft (labile or more polarizable) terminal ligands, having as a consequence a bigger change on their transition dipole moments. The trend related to the red-shift, as well as the ligand contribution to the arrival orbitals is the same for all chalcogenides in the $[Re_6(\mu_3\text{-}Q_8)X_6]^{4-}$ clusters, these results can be seen on the electronic supplementary information (ESI)† in Figures S1 and S2, as well in Tables S1 and S2.

All the excitation spectra mentioned before are similar, both in shape and intensity, due to all of them possess a high "core to core" character on the main electronic transitions. As was mentioned above, the shift toward the red region of the spectrum depends of the terminal ligand contribution to the arrival spinor. These can be corroborated analysing the results of the calculations of the absorption spectra for the bare-core (the $[Re_6(\mu_3\text{-}Q_8)]^{2+}$ core with out terminal ligands). In this case, when only the scalar relativistic effects were considered, three intense bands were appreciated at 434, 366 and 334 nm which are directly related to $t_{2g} \rightarrow t_{1u}$, $e_g \rightarrow t_{2u}$ and $t_{1u} \rightarrow e_g$ transitions respectively; the number of the bands increase with respect to the scalar calculation when the spin-orbit coupling were introduced, being the most intense those located at 500, 437, 394, 369 and 354 nm that can be characterized mainly as $u_{3/2u} \rightarrow u_{3/2g}$ and $u_{3/2u} \rightarrow e_{5/2g}$ for all the transitions. These bands for the bare-core have a similar assignation with the bands found for the $[Re_6(\mu_3\text{-}Q)_8X_6]^{4-}$ clusters with halide terminal ligands, the only difference is that these bands are shifted and also some of them are mixed with the increased of the terminal ligand contributions, as was mentioned on previous paragraph.

From this analysis we found a regularity for the composition of the absorption bands and also for the red-shift presented in all the halide complexes with respect to the $[Re_6(\mu_3\text{-}Q_8)]^{2+}$ core system. These are based fundamentally on the progressive increment of the terminal ligand contribution to the arrival orbitals of the main electronic transitions (as is observed in Table 1). This can suggest that the role of the terminal ligands is to modulate the intensity and position with the possibility to tune the absorption spectra into the NIR region.

The calculated spectra are in good agreement with the experimental data reported by Guilbaud *et al.* [10] for the $[Re_6(\mu_3\text{-}S_8)Cl_6]^{4-}$ cluster where a band was found around the 398.6 nm (3.11 eV) which corresponds to the experimental band at 380.3 nm (3.26 eV) and also with the results presented by Long *et al.* [19] for the $[Re_6(\mu_3\text{-}S_8)Br_6]^{4-}$ and the $[Re_6(\mu_3\text{-}S_8)\ I_6]^{4-}$ systems, where are our calculated transitions are located at 421.7 (2.94 eV) and 499.9 (2.48 eV), which correspond to the experimental values of 442.8 nm (2.80eV) and 508.1 nm (2.44 eV) for the $[Re_6(\mu_3\text{-}S_8)Br_6]^{4-}$ and $[Re_6(\mu_3\text{-}S_8)I_6]^{4-}$, respectively. For further information see Table 1.

Furthermore, when we change the chalcogenide ion instead of the terminal ligand, we also observed a bathochromic effect on the spectra possibly due to a heavy atom effect of the chalcogenide in the hexarhenium chalcogenide core, which produce an

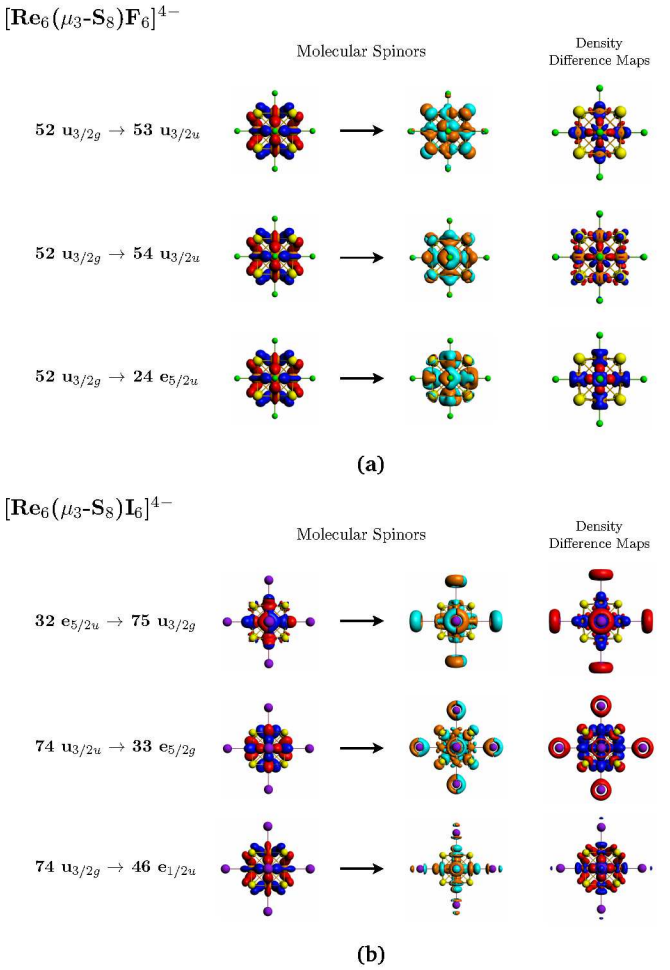

Fig. 3 Molecular spinor plots and electron density difference maps of the main electronic transitions involved on the absorption spectra for (a)$[Re_6(\mu_3\text{-}S_8)F_6]^{4-}$ and (b)$[Re_6(\mu_3\text{-}S_8)I_6]^{4-}$ complexes. The electron density difference maps were calculated as the difference of the final and initial molecular spinor densities for each electronic transitions, here we can identified depleted (red) or loaded (blue) zones with electron density during an electronic transition upon excitation

energetic rearrangement of the orbital and excitation energies moving these to a longer wavelengths regions as can be observed in Figure 4. Moreover, it is exhibited a decreased on calculated oscillator strengths in the following way: $S^{2-} > Se^{2-} > Te^{2-}$, this tendency is in agreement with the absorption intensities observed experimentally.[15]

2) σ-donor / π-acceptor Ligands

For the CN^- and NC^- π-acceptor ligands, the case where the donation and back donation phenomena is the same for both terminal ligands. We observed from Table 2, that the atomic orbital contribution to the molecular orbitals involved on the most important electronic transitions can be characterized as intra-core with certain ligand contribution. In this case, the ligand contribution is similar to those showed by fluoride and chloride ligands and on the region where also appears coincidently the spectra for the $[Re_6(\mu_3\text{-}S_8)CN_6]^{4-}$ and $[Re_6(\mu_3\text{-}S_8)\ NC_6]^{4-}$ complexes, as can be observed in Figure 5.

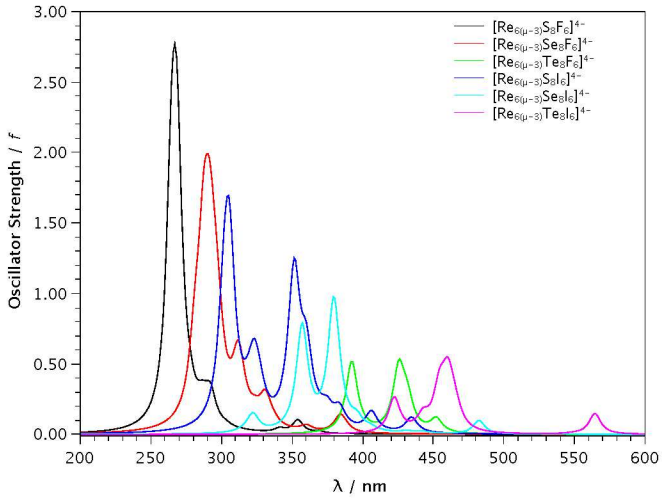

Fig. 4 Calculated excitation energies for the $[Re_6(\mu_3\text{-}S_8)X_6]^{4-}$ (Q = S^{2-}, Se^{2-}, Te^{2-} and X = F^-, I^-) cluster series at spin-orbit relativistic level with the SAOP functional in acetonitrile solvent.

Besides the shape of the spectra is quite similar there is a reduction on the absorption intensity (oscillator strength) when the terminal ligand is bonded to the rhenium core for the most π-acceptor atom, which is directly related to the lability of the σ-donor/π-acceptor ligands and their relative stability as was found in a previous work.[36] The same behaviour is observed for the -OCN^-/-NCO^- and -SCN^-/-NCS^- couples (See ESI, Figures S3 and S4). In the case of the OCN^-/NCO^- absorption spectra, as in the case of the halides and the CN^-/NC^- couple, these are directly related to the ligand participation on the orbitals involved on the electronic transitions; but for this couple of ligands both the departure and the arrival orbitals have a slight contribution of the terminal ligand atomic orbitals.

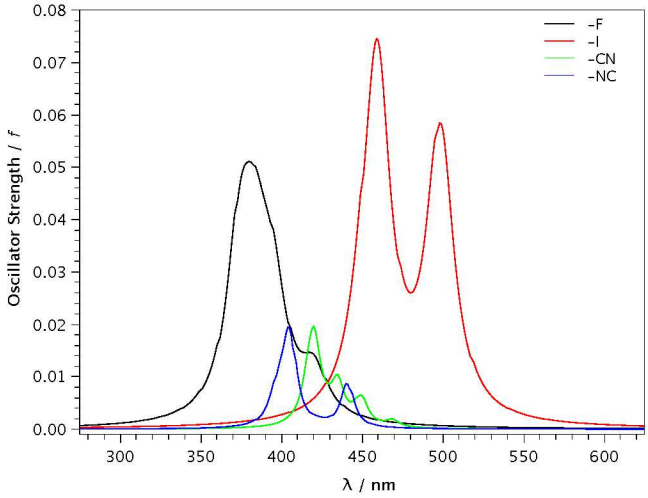

Fig. 5 Calculated excitation energies for the $[Re_6(\mu_3\text{-}S_8)X_6]^{4-}$ (X = F^-, I^-, CN^- and NC^-) cluster series at spin-orbit relativistic level with the SAOP functional in acetonitrile solvent.

Table 2 Excitation energies (eV), wavelengths (nm), oscillator strengths (*f*) and orbital assignation for the $[Re_6(\mu_3\text{-}S_8)X_6]^{4-}$ complexes (X = CN^-, NC^-, SCN^-, NCS^-, OCN^- and NCO^-) at spin-orbit relativistic level with the SAOP functional in acetonitrile solvent.

Band	Energy	λ	f(x100)	Active MOs	%	Assignation
$[Re_6(\mu_3\text{-}S_8)CN_6]^{4-}$						
a	2.95	420	0.4979	54 $u_{3/2u} \rightarrow$ 55 $u_{3/2g}$ 34 $e_{1/2u} \rightarrow$ 35 $e_{1/2g}$	67.35 20.46	Core - Core + 15.02% Lig.
b	2.85	435	0.2477	54 $u_{3/2u} \rightarrow$ 55 $u_{3/2g}$	92.52	Core - Core + 15.02% Lig.
c	2.76	449	0.1653	54 $u_{3/2g} \rightarrow$ 24 $e_{5/2u}$ 54 $u_{3/2g} \rightarrow$ 55 $u_{3/2u}$	75.03 15.85	Core + 11.55% Lig. - Core + 6.36% Lig.
$[Re_6(\mu_3\text{-}S_8)NC_6]^{4-}$						
a	3.06	405	0.5177	54 $u_{3/2u} \rightarrow$ 24 $e_{5/2g}$ 23 $e_{5/2u} \rightarrow$ 24 $e_{5/2g}$ 54 $u_{3/2g} \rightarrow$ 55 $u_{3/2u}$	55.87 26.90 12.62	Core + 12.03% Lig. - Core
b	2.81	441	0.2764	54 $u_{3/2g} \rightarrow$ 24 $e_{5/2u}$ 54 $u_{3/2g} \rightarrow$ 55 $u_{3/2u}$	62.12 21.06	Core - Core + 17.27% Lig.
$[Re_6(\mu_3\text{-}S_8)SCN_6]^{4-}$						
a	1.99	623	1.1585	62 $u_{3/2u} \rightarrow$ 63 $u_{3/2g}$	92.55	76.02% Lig. + Core - Core + 23.43% Lig.
b	1.83	677	3.1121	60 $u_{3/2g} \rightarrow$ 41 $e_{1/2u}$ 25 $e_{5/2u} \rightarrow$ 63 $u_{3/2g}$	49.43 46.66	58.64 % Lig. + Core - Core + 22.57% Lig.
c	1.67	741	0.8655	40 $e_{1/2g} \rightarrow$ 41 $e_{1/2u}$	94.75	68.05 % Lig. + Core - Core + 22.57% Lig.
$[Re_6(\mu_3\text{-}S_8)NCS_6]^{4-}$						
a	2.91	426	7.0899	40 $e_{1/2u} \rightarrow$ 41 $e_{1/2g}$ 61 $u_{3/2u} \rightarrow$ 26 $e_{5/2g}$ 61 $u_{3/2u} \rightarrow$ 41 $e_{1/2g}$	32.89 30.81 24.00	Core + 45.45% Lig. - Core + 21.57% Lig.
b	2.85	435	2.3586	25 $e_{5/2u} \rightarrow$ 63 $u_{3/2g}$ 61 $u_{3/2u} \rightarrow$ 41 $e_{1/2g}$	71.01 13.25	54.88% Lig. + Core - Core + 20.52% Lig.
$[Re_6(\mu_3\text{-}S_8)OCN_6]^{4-}$						
a	3.09	401	0.9786	58 $u_{3/2g} \rightarrow$ 59 $u_{3/2u}$	87.45	Core + 1.96% Lig. - Core + 6.64% Lig.
b	2.88	431	0.3483	24 $e_{5/2u} \rightarrow$ 25 $e_{5/2g}$ 58 $u_{3/2g} \rightarrow$ 59 $u_{3/2u}$	63.74 17.88	Core + 42.95% Lig. - Core
c	2.69	460	0.7868	58 $u_{3/2g} \rightarrow$ 38 $e_{1/2u}$	98.33	Core + 1.96% Lig. - Core + 7.76% Lig.
$[Re_6(\mu_3\text{-}S_8)NCO_6]^{4-}$						
a	3.15	393	1.5115	24 $e_{5/2u} \rightarrow$ 59 $u_{3/2g}$ 57 $u_{3/2u} \rightarrow$ 25 $e_{5/2g}$	71.95 12.25	Core + 35.15% Lig. - Core + 4.85% Lig.
b	2.77	448	0.2481	24 $e_{5/2u} \rightarrow$ 25 $e_{5/2g}$ 58 $u_{3/2g} \rightarrow$ 59 $u_{3/2u}$	68.27 12.27	Core + 1.96% Lig. - Core

This ligand contribution could modify the energetic gap among the orbitals involved on the electronic transitions, producing an energetic increment, and having as a consequence a blued-shift of the electronic spectra with respect to the CN^-/NC^- cluster pair as is observed in Figure 6. Finally, for the SCN^- and NCS^- terminal ligands the nature of the orbital involved on the electronic transition are significant different with respect to all the other σ-donor and π-acceptor terminal ligands. On this the ligand contribution is bigger than the core contribution for the departure orbitals and around 20% for the arrival orbitals.

We had determined in a previous work[36] the high electrophilic character of the $[Re_6(\mu_3\text{-}Q_8)]^{2+}$ core, for that reason the π-acceptor ligands, which withdraw electron density, destabilized the core orbitals. This destabilization can be traduced as a reduction of the frontier orbitals energy gap and this can lead to a strongest red-shift as in the case of the SCN^-. Within the Hard and Soft Acid-Base (HSAB) theory, the softest iodide ligand produce a destabilizing interaction with the hard and electrophilic rhenium chalcogenide core making this ligand the most labile in the halide series and which produce the maximum red-shift on the absorption spectra. For the thiocyante ligand the consequence of the red-shift is due to the back-donation to π^*-orbitals.

After the analysis of these results, and considering the experimental evidence of the luminescence reported for these clusters, we could suggest, based on the nature of the electronic transitions of the absorption spectra, that the emission spectra would have a

certain ligand to metal charge transfer (LMCT) character, which could modify the wavelength of the mentioned emission. In the same way the ligand and the chalcogenide effect could tune their emission.

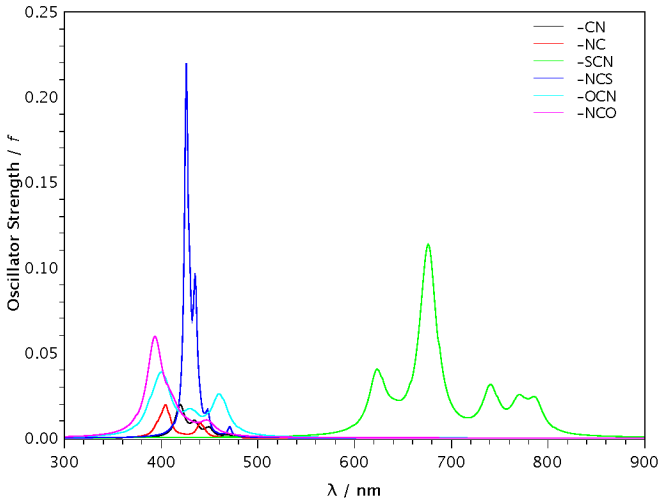

Fig. 6 Calculated excitation energies for the $[Re_6(\mu_3\text{-}S_8)X_6]^{4-}$ (X = CN^-, NC^-, SCN^-, NCS^-, OCN^- and NCO^-) cluster series at spin-orbit relativistic level with the SAOP functional in acetonitrile solvent.

4 Conclusions

The most labile (or electron-withdrawing) ligands produce a reduction of the energy-gap with respect to the $[Re_6(\mu_3\text{-}Q_8)]^{2+}$ core, this crystal field effect produced a red-shift in the absorption spectra for all the $[Re_6(\mu_3\text{-}Q_8)X_6]^{4-}$ complexes, where this shift is bigger when more labile (or electron-withdrawing) is the terminal ligand. In all the cases, we found two characteristic bands centred in 300 and 450 nm, where the position of these bands are directly determined by the terminal ligand. The only two exceptions are the SCN^- and NCS^- cases. In both cases the molecular spinors involved in the main electronic transitions are entirely localized over the SCN^- or NCS^- fragments, this produce the strongest red-shift for the series of complexes having absorption bands on the NIR region.

In general the variation of the absorption spectra of these clusters (with exception of the SCN^-/NCS^-) is not significant when different terminal ligands are used. This allowed us the possibility to compare the absorption spectra of the $[Re_6(\mu_3\text{-}Q_8)X_6]^{4-}$ substituted complexes versus the absorption spectra of the $[Re_6(\mu_3\text{-}Q_8)]^{2+}$ core, showing the possibility of tuning the absorption spectra via ligand field modification of the orbital energetics of the rhenium chalcogenide core.

As work perspective, we plan to continue the study of the optical properties of these clusters and also to understand the nature of the excited states involved on their luminescence. This can allow us to predict theoretically the emission spectra for these systems and also to find any connection between the absorption and emission spectra. For now, we only could suggest that even these clusters are substituted by different terminal ligands, the absorption spectra remains relatively constant. From this, we could expect that the emission spectra of these heavy-element containing clusters probably have also relatively constant bands. If this is true, this could be very significant from technological point of view specially for the development of sensing technologies.

5 Acknowledgements

This work has been supported by the Grant Millennium N° RC120001 adn the Projects FONDECYT N° 1150629, FONDECYT N° 11140294 and the AKA-FINLAND-CONICYT-CHILE 2012. J.A.M.L. acknowledges CONICYT/ Postdoctorado FONDECYT N° 3150041. W.A.R.L. acknowledges CONICYT/PCHA/Doctorado Nacional/2013 N° 63130118 for his Ph.D. fellowship.

References

1 R. Chevrel, M. Sergent and J. Prigent, *J. Solid State Chem.*, 1971, 515.
2 J.-C. P. Gabriel, K. Boubekeur, S. Uriel and P. Batail, *Chem. Rev.*, 2001, **101**, 2037–2066.
3 A. W. Maverick and H. B. Gray, *J. Am. Chem. Soc.*, 1981, **103**, 1298–1300.
4 A. W. Maverick, J. S. Najdzionek, D. MacKenzie, D. G. Nocera and H. B. Gray, *J. Am. Chem. Soc.*, 1983, **105**, 1878–1882.
5 B. K. Roland, W. H. Flora, H. D. Selby, N. R. Armstrong and Z. Zheng, *J. Am. Chem. Soc.*, 2006, **128**, 6620–6625.
6 L. F. Szczepura, D. L. Cedeño, D. B. Johnson, R. McDonald, S. A. Knott, K. M. Jeans and J. L. Durham, *Inorg. Chem.*, 2010, **49**, 11386–11394.
7 T. Yoshimura, T. Ikai, T. Takayama, T. Sekine, Y. Kino and A. Shinohara, *Inorg. Chem.*, 2010, **49**, 5876–5882.
8 T. Yoshimura, S. Ishizaka, Y. Sasaki, H.-B. Kim, N. Kitamura, N. G. Naumov and V. E. Sokolov, Maxim N.; Fedorov, *Chem. Lett.*, 1999, **28**, 1121–1122.
9 T. Yoshimura, S. Ishizaka, K. Umakochi, Y. Sasaki, H.-B. Kim and N. Kitamura, *Chem. Lett.*, 1999, 697.
10 C. Guilbaud, A. Deluzet, B. Domercq, P. Molinié, C. Coulon, K. Boubekeur and P. Batail, *Chem. Commun*, 1999, **18**, 1867–1868.
11 T. G. Gray, C. M. Rudzinski, D. G. Nocera and R. Holm, *Inorg. Chem.*, 1999, **38**, 5932–5933.
12 T. Yoshimura, Z.-N. Chen, A. Itasaka, M. Abe, Y. Sasaki, S. Ishizaka and N. Kitamura, *Inorg. Chem.*, 2003, **42**, 4857–4863.
13 Y. Molard, A. Ledneva, M. Amela-Cortes, V. Cîrcu, N. G. Naumov, C. Mériadec, F. Artzner and S. Cordier, *Chem. Mater*, 2011, **23**, 5122–5130.
14 W. B. Wilson, K. Stark, D. B. Johnson, Y. Ren, H. Ishida, D. L. Cedeño and L. F. Szczepura, *Eur. J. Inorg. Chem.*, 2014, **2014**, 2254–2261.
15 T. G. Gray, C. M. Rudzinski, E. E. Meyer, R. H. Holm and D. G. Nocera, *J. Am. Chem. Soc.*, 2003, **125**, 4755–4770.
16 N. Kitamura, Y. Ueda, S. Ishizaka, K. Yamada, M. Aniya and Y. Sasaki, *Inorg. Chem.*, 2005, **44**, 6308–6313.
17 K. A. Brylev, Y. V. Mironov, S. S. Yarovoi, N. G. Naumov, V. E. Fedorov, S.-J. Kim, N. Kitamura, Y. Kuwahara, K. Yamada, S. Ishizaka and Y. Sasaki, *Inorg. Chem.*, 2007, **46**, 7414–7422.
18 M. A. Shestopalov, K. E. Zubareva, O. P. Khripko, Y. I. Khripko, A. O. Solovieva, N. V. Kuratieva, Y. V. Mironov, N. Kitamura, V. E. Fedorov and K. A. Brylev, *Inorg. Chem.*, 2014, **53**, 9006–9013.
19 J. R. Long, L. S. McCarty and R. H. Holm, *J. Am. Chem. Soc.*, 1996, **118**, 4603–4616.
20 L. G. Beauvais, M. P. Shores and J. R. Long, *Chem. Mater*, 1998, **10**, 3783–3786.
21 H. D. Selby, B. K. Roland and Z. Zheng, *Acc. Chem. Res.*, 2003, **36**, 933–944.
22 N. Ding, G. S. Armatas and M. G. Kanatzidis, *J. Am. Chem. Soc.*, 2010, **132**, 6728–6734.

23 X. Yuan, B. Zhang, Z. Luo, Q. Yao, D. T. Leong, N. Yan and J. Xie, *Angew. Chem. Int. Ed.*, 2014, **53**, 4623–4627.

24 W. C. Corbin, G. S. Nichol and Z. Zheng, *J. Clust. Sci*, 2014, **26**, 279–290.

25 L. Alvarez-Thon, L. Hernández-Acevedo and R. Arratia-Pérez, *J. Chem. Phys.*, 2001, **115**, 726–730.

26 A. Deluzet, H. Duclusaud, P. Sautet and S. A. Borshch, *Inorg. Chem.*, 2002, **41**, 2537–2542.

27 E. G. Tulsky, N. R. M. Crawford, S. A. Baudron, P. Batail and J. R. Long, *J. Am. Chem. Soc.*, 2003, **125**, 15543–15553.

28 T. Aubert, A. Y. Ledneva, F. Grasset, K. Kimoto, N. G. Naumov, Y. Molard, N. Saito, H. Haneda and S. Cordier, *Langmuir*, 2010, **26**, 18512–18518.

29 C. Echeverría, A. Becerra, F. Nuñez-Villena, A. Muñoz-Castro, J. Stehberg, Z. Zheng, R. Arratia-Pérez, F. Simon and R. Ramirez-Tagle, *New. J. Chem.*, 2012, **36**, 927–932.

30 R. Arratia-Pérez and L. Hernández-Acevedo, *J. Chem. Phys.*, 1999, **110**, 2529–2532.

31 R. Arratia-Pérez and L. Hernández-Acevedo, *J. Chem. Phys.*, 1999, **111**, 168–172.

32 R. Arratia-Pérez and L. Hernández-Acevedo, *J. Chem. Phys.*, 2003, **118**, 7425–7430.

33 M. W. Willer, J. R. Long, C. C. McLauchlan and R. H. Holm, *Inorg. Chem.*, 1998, **37**, 328–333.

34 X. Tu, G. S. Nichol, P. Keng, J. Pyun and Z. Zheng, *Macromolecules*, 2012, **45**, 2614–2618.

35 Z. Zheng, J. R. Long and R. H. Holm, *J. Am. Chem. Soc.*, 1997, **119**, 2163–2171.

36 W. A. Rabanal León, J. A. Murillo-López, D. Páez Hernández and R. Arratia-Pérez, *J. Phys. Chem. A*, 2014, **118**, 11083–11089.

37 G. Te Velde, F. M. Bickelhaupt, E. J. Baerends, C. Fonseca Guerra, S. J. A. Van Gisbergen, J. G. Snijders and T. Ziegler, *Amsterdam Density Functional (ADF) Program: DFT for molecules*, 2012.

38 E. Van Lenthe, J. G. Snijders and E. J. Baerends, *J. Chem. Phys.*, 1996, **105**, 6505–6516.

39 M. Filatov and D. Cremer, *Molecular Physics*, 2003, **101**, 2295–2302.

40 A. A. Opalovskii, V. E. Fedorov and E. U. Lobkov, *Russ. J. Inor. Chem.*, 1971, **16**, 790.

41 A. A. Opalovskii, V. E. Fedorov, E. U. Lobkov and B. G. Erenburg, *Russ. J. Inor. Chem.*, 1971, **16**, 1685.

42 Y. V. Mironov, J. A. Cody, T. E. Albrecht-Schmitt and J. A. Ibers, *J. Am. Chem. Soc.*, 1997, **119**, 493–498.

43 L. Leduc, A. Perrin and M. Sergent, *C.R. Acad. Sci. Paris, Ser. II*, 1983, **296**, 961.

44 M. A. L. Marques and E. K. U. Gross, *Annu. Rev. Phys. Chem.*, 2004, **55**, 427–455.

45 S. J. A. Van Gisbergen, J. G. Snijders and E. J. Baerends, *Computer Physics Communications*, 1999, **118**, 119–138.

46 O. V. Gritsenko, P. R. T. Schipper and E. J. Baerends, *Chem. Phys. Lett.*, 1999, **302**, 199–207.

47 C. C. Pye and T. Ziegler, *Theo. Chem. Acc.*, 1999, **101**, 396.

48 A. Klamt, *J. Chem. Phys.*, 1995, **99**, 2224.

49 E. Van Lenthe and E. J. Baerends, *J. Comput. Chem.*, 2003, **24**, 1142–1156.